Journal of Hazardous Materials 209–210 (2012) 193–198

Contents lists available at SciVerse ScienceDirect

Journal of Hazardous Materials

journal homepage: www.elsevier.com/locate/jhazmat

Modifying Fe_3O_4 nanoparticles with humic acid for removal of Rhodamine B in water

Liang Peng[a,b,*], Pufeng Qin[a,**], Ming Lei[a], Qingru Zeng[a], Huijuan Song[a,b], Jiao Yang[a], Jihai Shao[a], Bohan Liao[a], Jidong Gu[a,c]

[a] Department of Environmental Science & Engineering, Hunan Agricultural University, Changsha 410128, PR China
[b] School of Metallurgical Science and Technology, Central South University, Changsha 410083, PR China
[c] Laboratory of Environmental Toxicology, School of Biological Sciences, The University of Hong Kong, Pokfulam Road, Hong Kong SAR, Hong Kong, China

ARTICLE INFO

Article history:
Received 4 October 2011
Received in revised form
29 December 2011
Accepted 3 January 2012
Available online 11 January 2012

Keywords:
Nano-Fe_3O_4
Rhodamine B
Nanostructure
Separations
Adsorption
Interface

ABSTRACT

Humic acid (HA) modifying Fe_3O_4 nanoparticles (Fe_3O_4/HA) was developed for removal of Rhodamine B from water. Fe_3O_4/HA was prepared by a coprecipitation procedure with cheap and environmentally friendly iron salts and HA. TEM images revealed the Fe_3O_4/HA (with ~10 nm Fe_3O_4 cores) were aggregated as aqueous suspensions. With a saturation magnetization of 61.2 emu/g, the Fe_3O_4/HA could be simply recovered from water with magnetic separations at low magnetic field gradients within a few minutes. Sorption of the Rhodamine B to Fe_3O_4/HA reached equilibrium in less than 15 min, and agreed well to the Langmuir adsorption model with maximum adsorption capacities of 161.8 mg/g. The Fe_3O_4/HA was able to remove over 98.5% of Rhodamin B in water at optimized pH.

1. Introduction

Color is the first contaminant to be recognized in water and has to be removed from wastewater before discharging it into water bodies. Color impedes light penetration, retards photosynthetic activity, inhibits the growth of biota and also has a tendency to chelate metal ions which result in micro-toxicity to fish and other organisms [1]. Residual dyes are the major contributors to color in wastewaters generated from textile and dye manufacturing industries, etc. [2]. It should be noted that the contamination of drinking water by dyes at even a concentration of 1.0 mg/L could impart significant color, making it unfit for human consumption [2]. Therefore, it is significant in environmental science to investigate the removal of dye from water body.

Currently, several physical or chemical processes are used to treat dye-laden wastewaters, such as adsorption [3–5], chemical oxidation [6], electrochemical oxidation [7], and photocatalytic oxidation [8]. Most of dyes are stable to photo-degradation, bio-degradation and oxidizing agents [2]. Therefore, the adsorption process is one of the high efficient, low-cost methods to remove dyes from water. Gad et al. [3] utilized activated carbon fabricated from agricultural by-products bagasse pith for the removal of Rhodamine B (RhB). This technique not only removes the dye but also disposes the agricultural castoff. However, an extreme variability in their composition arising from the use of these low-cost organic adsorbents affects the yield of the adsorption and hence the operating conditions. Ma et al. [9] fabricated carboxylmethylcellulose grafting cationic polyacrylamide (CMC-g-CPAM) with quaternary ammonium group which was used to adsorb active dyes. The resin features high removal efficiency on active dyes by means of adsorption, bridging and flocculation. The decolorizing rate is up to 91–98%. However, the complicated preparation restricts its application. The mineral such as vermiculite [10], kaolinite [11], and bentonite [12] was developed as adsorbent materials for removal of RhB from water as well. However, these materials are difficult to re-collect from water and cannot be used to treat the wide range of dye-laden wastewater effectively.

Magnetic nanomaterials are suitable for removal of dye from lake and river, because it can be re-collected from water conveniently. Bare magnetite nanoparticles are susceptible to air oxidation [13] and easily aggregated in aqueous systems. The silica is usually coated at the Fe_3O_4 as protective reagent and then the function group is grafted at the surface of silica [14]. Recently, some

* Corresponding author at: College of Resource and Environment, Hunan Agricultural University, Changsha 410128, PR China. Tel.: +86 731 84673620.
** Corresponding author.
E-mail addresses: pengliang@hunau.net, pengliang2004@126.com (L. Peng), Qinpft@163.com (P. Qin).

0304-3894/$ – see front matter © 2012 Elsevier B.V. All rights reserved.
doi:10.1016/j.jhazmat.2012.01.011

organic substances such as oleic acid (OA) and ethylenediaminetetraacetic acid (EDTA) [15] have been coated at Fe_3O_4 nanoparticles as stable matters for nanoparticles and their function groups have adsorptive effect on heavy metal. Recent research indicates that humic acid (HA) has high affinity to Fe_3O_4 nanoparticles, and the sorption of HA on Fe_3O_4 nanoparticles enhances the stability of nanomaterial by preventing being oxidation [16,17]. Furthermore, the HA on Fe_3O_4 enhances the sorption of RhB, because the negative charge of HA improves adsorbing RhB with positive charge.

In this study, a novel low-cost magnetic sorbent material prepared by modifying Fe_3O_4 magnetic nanoparticles with HA was developed for removal of RhB from water. The physical and chemical characterization of the synthesized HA modified Fe_3O_4 nanoparticles (Fe_3O_4/HA) was conducted, and the applicability of Fe_3O_4/HA in RhB removal was evaluated in view of the sorption kinetic and capacity, effects of pH, as well as the adsorbent dosage.

2. Experimental

2.1. Preparation and characterization of magnetic nanomaterials

HA coated Fe_3O_4 magnetic nanoparticles were synthesized with methods modified from Ref. [18]. Briefly, 6.1 g of $FeCl_3{\cdot}6H_2O$ (Sinopharm Chemical Reagent Co. Ltd., AR) and 4.2 g of $FeSO_4{\cdot}7H_2O$ (Sinopharm Chemical Reagent Co. Ltd., AR) were dissolved in 100 mL water and heated to 90 °C, then two solutions, 10 mL of ammonium hydroxide (25%) (Sinopharm Chemical Reagent Co. Ltd., AR) and 0.5 g of humic acid sodium salt (Shanghai Chemical Reagent Co. Ltd., AR) dissolved in 50 mL of water, were added rapidly and sequentially. The mixture was stirred at 90 °C for 30 min and then cooled to room temperature. The black substance was collected by centrifugation and washed to neutral with water. The obtained black precipitate was Fe_3O_4/HA nanoparticles. The bare Fe_3O_4 was prepared with the same method as that of Fe_3O_4/HA, except with the no HA was added.

Transmission electron microscopy (TEM) was carried out with H-7500 (JEM-1230(HC), Japan). The BET (N_2) surface areas of materials were measured with NOVA 1000 (USA). The zeta potential of Fe_3O_4/HA particles were measured at various pH with a DELSA 440SX (USA).

2.2. Procedure of RhB sorption

50 mg of prepared Fe_3O_4/HA was added into a 100 mL of mixed solution containing 50 mg/L RhB (Beijing Chemical Reagent Co. Ltd., AR), the mixture was adjusted to pH 6.0 with HCl (Tianjing Chemical Reagent Co. Ltd., AR) or NaOH (Tianjing Chemical Reagent Co. Ltd., AR) and stirred for 30 min. Then the magnetic Fe_3O_4/HA with sorbed RhB was separated from the mixture with a permanent hand-held magnet. The residual RhB in the solution was determined with 721 spectrophotometer (Jinke, China) at the wavelength of 554 nm. For achieving the adsorption isotherms of the RhB, solutions with varying initial dye concentration were treated with the same procedure as above at room temperature (20 °C).

3. Results and discussion

3.1. Characterization of Fe_3O_4/HA

Spectroscopic analysis showed the successful coating of HA on the Fe_3O_4 surface. Infrared spectrum (Fig. 1) showed the C=O stretches of Fe_3O_4/HA at ~1639 cm^{-1}, indicating the carboxylate anion interacting with the FeO surface, as the C=O stretches in free

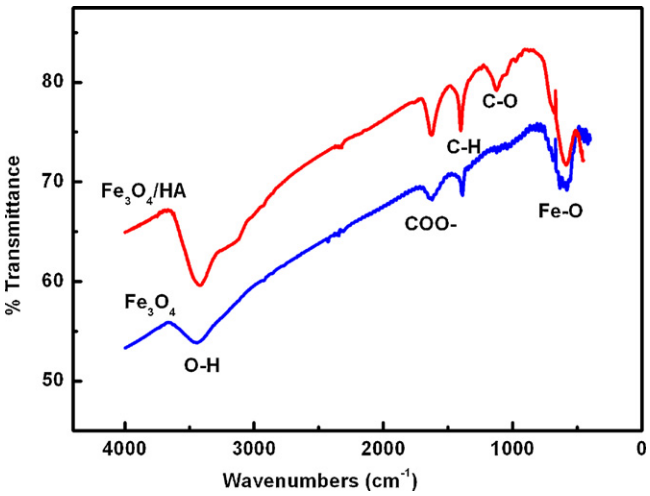

Fig. 1. FT-IR spectra of Fe_3O_4/HA and Fe_3O_4 nanoparticles.

carboxylic acid was above 1700 cm^{-1} [19]. The band at 1402 cm^{-1} was most likely due to the CH_2 scissoring. The 1116 cm^{-1} was the C—O stretches of COO^-. For the bare Fe_3O_4 materials, however, the weakly C=O stretches was observed, and no C—O stretches in found, suggesting the binding of HA to Fe_3O_4. It is generally believed the binding of HA to Fe_3O_4 surface is mainly through ligand exchange [20].

The zeta potentials of the as-prepared Fe_3O_4/HA were measured at varied pH and shown in Fig. 2. The pH_{PZC} of Fe_3O_4/HA decreased to ~2.3 since the coated HA had abundant carboxylic acid groups. The zeta potential of gray humic acid is negatively charged in the range of pH 0.5–9.0 [21]. The low pH_{PZC} indicates that the Fe_3O_4/HA are negatively charged at the entire environmentally relevant acidity (pH 3–9), which prohibits the aggregation of Fe_3O_4/HA and benefits the sorption of positively charged substance.

The saturation magnetizations of Fe_3O_4/HA was 61.2 emu/g (Fig. 3). Separation of Fe_3O_4/HA from its aqueous dispersions can be easily finished in a few minutes with permanent handheld magnet. Fig. 3 shows the dispersive Fe_3O_4/HA was aggregated under the handheld magnet and then was re-dispersed in solution. The black aqueous suspensions of bare Fe_3O_4 nanoparticles were easily oxidized to brown suspensions without magnetization, whereas no significant change of the saturation magnetization and color was observed after the Fe_3O_4/HA was stored in water for one

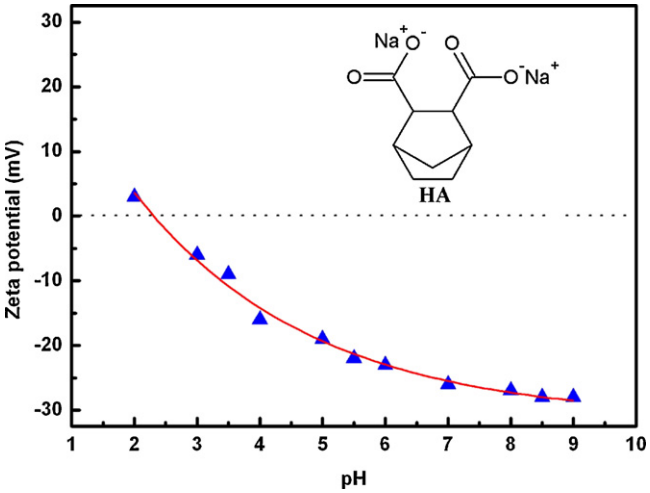

Fig. 2. The zeta potentials of the as-prepared Fe_3O_4/HA nanoparticles (the insert is the molecular from of humic acid sodium).

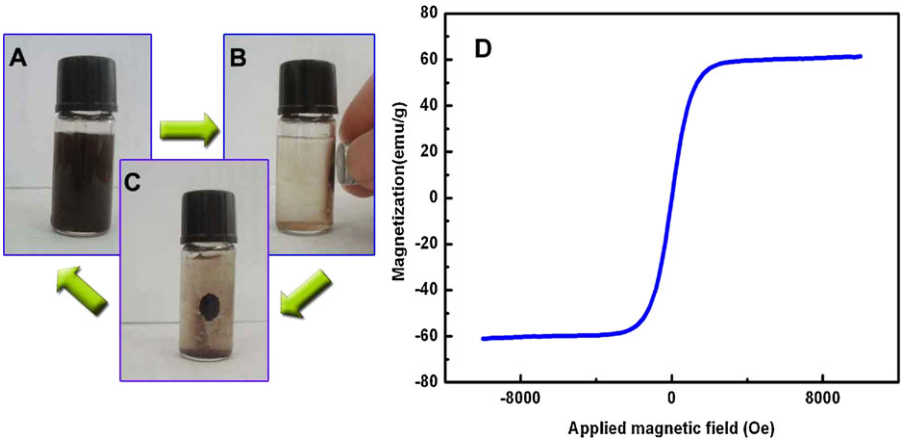

Fig. 3. (A) Dispersive Fe_3O_4/HA solution; (B) Fe_3O_4/HA solution in magnetic field of hand-hold magnets; (C) aggregative Fe_3O_4/HA; (D) magnetization curves of the as-prepared Fe_3O_4/HA nanoparticles.

month, indicating the HA coating was able to maintain the saturation magnetization of Fe_3O_4/HA nanoparticles by prohibiting their oxidation.

BET analysis revealed the surface area for Fe_3O_4/HA was 64 m^2/g. This low value of surface area might be attributed to HA had highly narrow microporosity which adsorbs no N_2 at 77 K. It was reported that the measured surface area of humic substances was 42.5 m^2/g with CO_2 at 273 K, but less than 1 m^2/g with N_2 at 77 K [22].

The TEM image of the as-prepared Fe_3O_4/HA was shown in Fig. 4. The core of the Fe_3O_4 magnetic nanoparticle had a typical size ~10 nm, but the entire Fe_3O_4/HA particles contained aggregates with no uniform size and fractal feature. Likewise, Ills et al. [17] also observed that Fe_3O_4 particles with a primary size of ~10 nm aggregated to form nonuniform size and fractal aggregates with an average size of ~120 nm in sol solutions containing HA. The aqueous suspensions of the as-prepared Fe_3O_4 particles had larger average value (250 nm) and wider range of hydrodynamic size (160–366 nm) than those of Fe_3O_4/HA (140 nm, 104–189 nm) though these two materials have almost the same primary size. These results clearly demonstrate that coating Fe_3O_4 nanoparticles with HA efficiently reduces their aggregation.

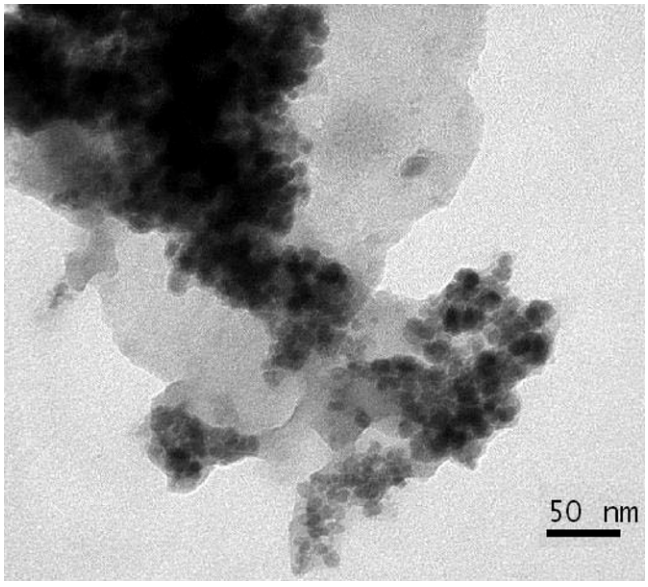

Fig. 4. TEM of Fe_3O_4/HA nanoparticle.

3.2. Sorption kinetics

The sorption dynamics of RhB to Fe_3O_4/HA were evaluated by adding 50 mg of the as-obtained Fe_3O_4/HA into 100 mL of a mixed solution containing 50 mg/L RhB (pH 6.0) at room temperature. The concentration of RhB in solution was measured using 721 spectrophotometer, after the Fe_3O_4/HA adsorption was taken for 15 min, 30 min, 45 min, 60 min, 75 min, 90 min, 105 min, and 120 min. Results (Fig. 5) showed that sorption equilibrium was reached in ~15 min, which was longer than those in fly ash sorption with Fenton pre-oxidation [4] but shorter than those in active carbon (~2 h) [3]. The slow kinetics are likely due to saturation of the outer binding sites and slow site-site exchange of RhB because of the disordered structure of the HA layer in Fe_3O_4/HA. The pseudo first-order model was employed to perform the kinetics study. The linear form of the pseudo first-order rate expression was given as Eq. (1):

$$\ln(q_e - q_t) = \ln\ q_e - kt \quad (1)$$

where k (min^{-1}) is the rate constant of the pseudo first-order adsorption, q_e is the equilibrium adsorption capacity (mg/g), q_t is instantaneous adsorption capacity (mg/g). The correlation coefficient (R^2) is 0.997, reveals that the pseudo first-order model is validity for this adsorption process. The k is 0.189 min^{-1}, and q_e is 81.5 mg/g.

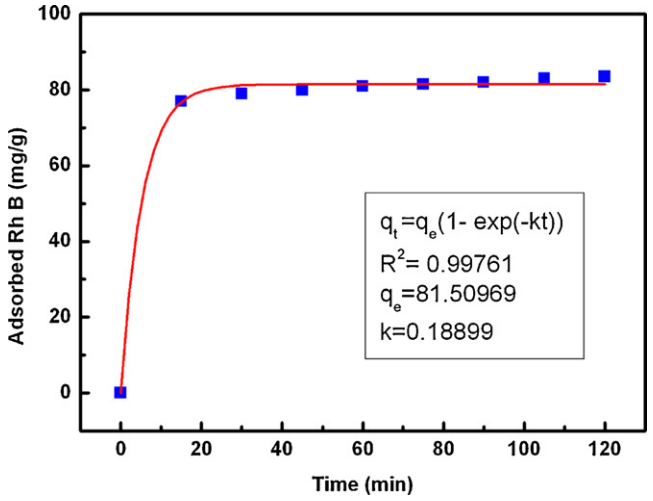

Fig. 5. Kinetics graph for removal of RhB by Fe_3O_4/HA.

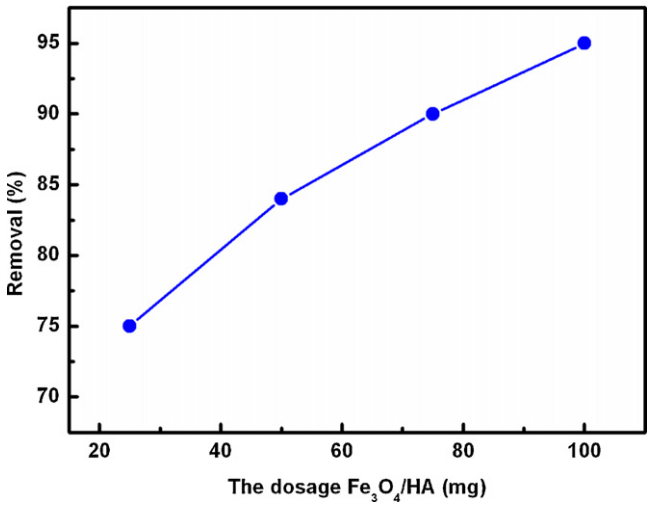

Fig. 6. The influence of adsorbent dosage on removal rate of RhB.

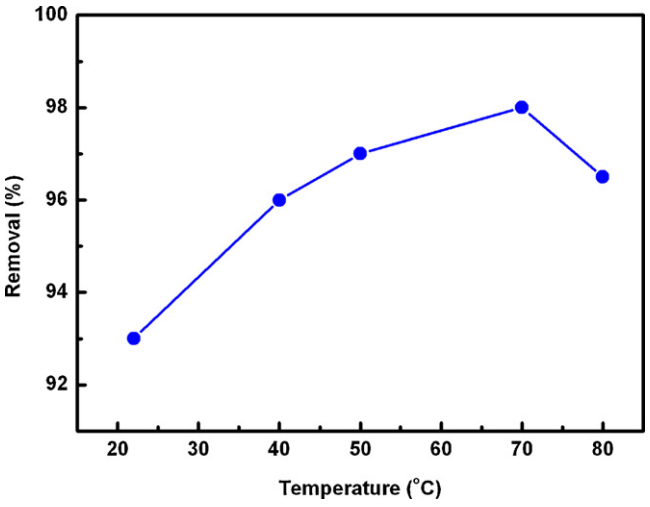

Fig. 9. The influence of temperature on RhB removal rate by Fe_3O_4/HA.

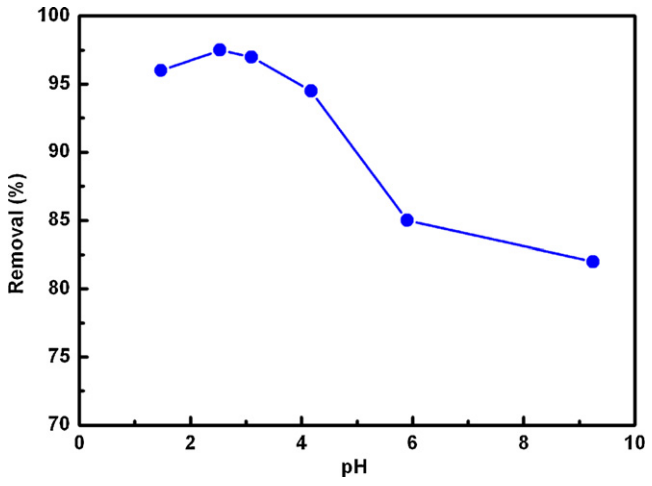

Fig. 7. The effect of pH on removal efficiency of 50 mg/L RhB by Fe_3O_4/HA.

3.3. Effect of dosage

The effect of Fe_3O_4/HA dosage on removal of RhB is investigated and shown in Fig. 6. Fe_3O_4/HA of 25 mg, 50 mg, 75 mg, and 100 mg was taken in 100 mL solution of 50 mg/L RhB, respectively. It is revealed that the removal efficiency of RhB increase as increasing the absorbent dosage. The 25 mg Fe_3O_4/HA got removal efficiency of 75%, while 100 mg Fe_3O_4/HA got removal efficiency of 95%.

3.4. Effect of pH

The effect of pH on the adsorption of RhB ions onto Fe_3O_4/HA is shown in Fig. 7, where 50 mg Fe_3O_4/HA was utilized to adsorb 50 mg/L RhB in100 mL solution. The pH of solution was adjusted by HCl or NaOH and all pH measurements were carried out using digital pH meter. The HCl of 30.0, 3.0, 1.0 and 0.1 mmol was added to solution, the pH was adjusted to 1.5, 2.5, 3.1 and 4.0, respectively. The 0.1 mmol NaOH was added to solution, the pH was adjusted to 9.25. The results showed the highest removal efficiency of RhB at pH 2.53, as much as 98.5%. At pH 3.10 the removal efficiency was 97%. At pH 9.25 the RhB removal efficiency was 82%. The sorption of RhB on the surface of the Fe_3O_4/HA is significantly influenced by the pH. It is attributed to that a change in pH of the solution results in forming different ionic species and different surface charge of Fe_3O_4/HA. When pH lower than the pH_{PZC} of Fe_3O_4/HA (~2.3), the surface of Fe_3O_4/HA is positive and has weakly interaction with RhB cation. When the pH higher than the pH_{PZC} of Fe_3O_4/HA, the surface of Fe_3O_4/HA is negative, because the carboxylic acids in HA form carboxylate ions (anionic species). And then it increased the removal efficiency of the RhB of cationic form [23]. However, when the pH is higher than 4, the zwitterionic form of RhB in water (Fig. 8) decreases the removal efficiency of RhB. Consequently, the removal efficiency would decrease sharply when the pH is higher than ~4.0.

3.5. Effect of temperature

The 50 mg Fe_3O_4/HA was taken in 100 mL solution with 50 mg/L RhB and oscillated for 100 min at different temperatures. The plot of removal efficiency as a function of temperature is shown in Fig. 9.

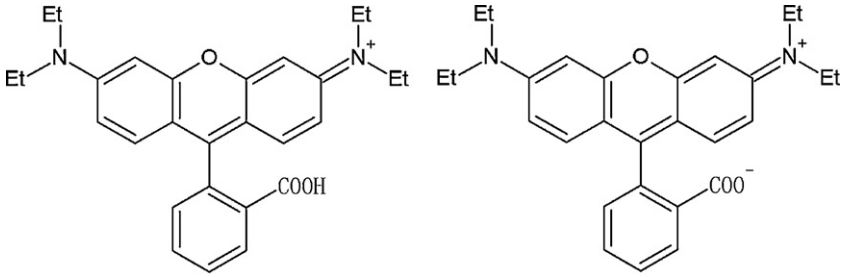

Fig. 8. Molecular from of RhB (cationic and zwitterionic forms).

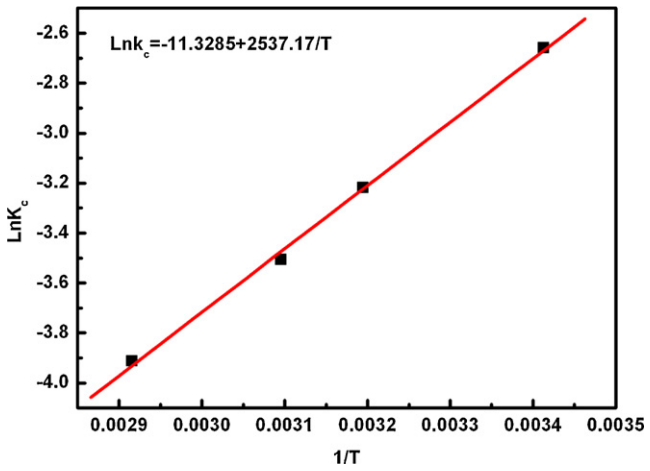

Fig. 10. Plot of ln k_C against reciprocal temperature for RhB sorption onto Fe_3O_4/HA.

It was revealed that the removal efficiency of RhB increased as the temperature increasing from 20 to 70 °C and then decreased as the temperature was higher than 70 °C. It is indicated that the removal efficiency depends on the temperature. The adsorptive HA on Fe_3O_4 is porosity, and their pore size is very small. Therefore, after the pore has the adsorbed RhB molecules at the opening, it will hinder the subsequent entrance of RhB molecules. The intra-particle diffusion rate of sorbate into the pores will be intensified as temperature increases, as diffusion is an endothermic process. However, the removal rate decreases as temperature higher than 70 °C. It may be attributed to the high temperature breaks the interaction of RhB and HA.

3.6. Thermodynamic studies

The uptake of RhB by the Fe_3O_4/HA increases on raising the temperature confirming the endothermic nature of the adsorption step. The change in standard free energy (ΔG°), enthalpy (ΔH°) and entropy (ΔS°) of adsorption is calculated from Eq. (2):

$$\Delta G = -RT\ln K_C \quad (2)$$

where R is the gas constant, K_C is the equilibrium constant and T is the temperature in K. The K_C value is calculated from Eq. (3):

$$K_C = \frac{C_A}{C_S} \quad (3)$$

where C_A and C_S are the equilibrium concentrations of dye ions on adsorbent (mg L^{-1}) and in the solution (mg L^{-1}), respectively. Standard enthalpy (ΔH) and entropy (ΔH°), of adsorption can be estimated from van't Hoff equation given in:

$$\ln K_C = \frac{-\Delta H}{RT} + \frac{\Delta S}{R} \quad (4)$$

The slope and intercept of the van't Hoff plot is equal to $-\Delta H/R$ and $\Delta S/R$, respectively [24]. The van't Hoff plot for the adsorption of RhB onto Fe_3O_4/HA is given in Fig. 10. Thermodynamic parameters obtained are summarized in Table 1. From Table 1, the negative values of enthalpy change ($\Delta H = -7.27$ kJ mol^{-1}) conforms

Table 1
The thermodynamic parameters of the adsorption of RhB using Fe_3O_4/HA.

Temperature (K)	$-\Delta G$ (kJ mol^{-1})	ΔH (kJ mol^{-1})	ΔS (J mol^{-1} K^{-1})
293	2.23	−7.27	−32.48
313	2.89		
323	3.25		
343	3.85		

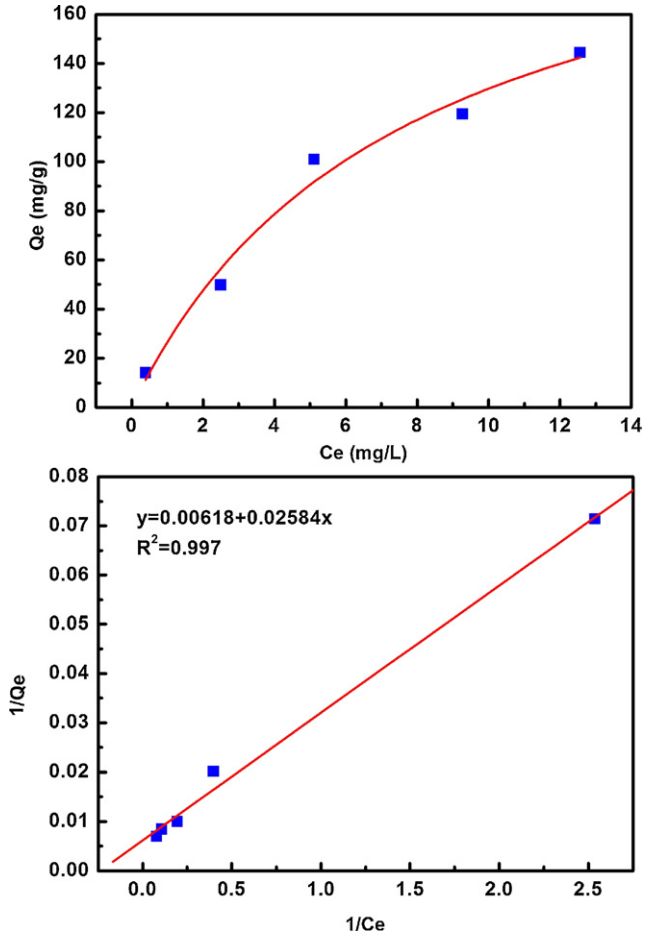

Fig. 11. Adsorption isotherms of RhB on Fe_3O_4/HA and the linear transformation of equilibrium adsorption data. (a) Adsorption isotherms and (b) linear from of Langmuir equation of adsorption of RhB.

the exothermic nature of the adsorption process. The negative value of ΔS ($\Delta S = -32.48$ J mol^{-1} K^{-1}) reflects the affinity of adsorbent material towards RhB. The spontaneity of the adsorption process is increased in the Gibbs energy of the system. The ΔG values vary in range with the mean values showing a gradual increase from −2.23 to −3.85 (kJ mol^{-1}) in the temperature range of 20–70 °C.

3.7. Sorption isotherms

The adsorption capacities of the as-obtained Fe_3O_4/HA to dye were measured individually at pH 6.0 with 0.5 g/L of Fe_3O_4/HA and varied RhB concentration, and the data of the dye adsorbed at equilibrium (q_e, mg/g) and the equilibrium dye concentration (C_e, mg/L) were fitted to the linear form of Langmuir adsorption model

$$\frac{C_e}{q_e} = \frac{1}{bq_m} + \frac{C_e}{q_m} \quad (5)$$

where q_m is the maximum adsorption capacity corresponding to complete monolayer coverage and b is the equilibrium constant (L/mg). The result is shown in Fig. 11. The data fit well to the model with correlation coefficients (r^2) in the range of 0.997, and the maximum adsorption capacity of 161.8 mg/g for RhB.

3.8. Regeneration and reuse

The reusability of adsorbents is of great importance as a cost effective process in water treatment. For the environmental sustainability of an adsorbent, a high regeneration capacity would add

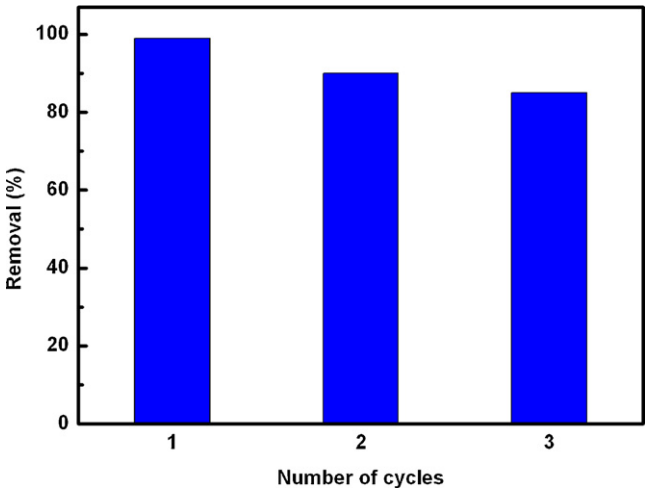

Fig. 12. Removal efficiency of regenerating Fe_3O_4/HA on RhB in pH 2.5.

value to the water treatment. In order to regenerate and reuse the Fe_3O_4/HA after adsorbing RhB, the 1.0 M HCl was selected as the regeneration agent. Three cycles of adsorption–desorption studies were accordingly carried out. As shown in Fig. 12, the removal rate was 98% at the first cycle. After first cycle, the adsorption capacity of RhB was reduced by nearly 8%, which was due to the incomplete desorption of RhB. After three consecutive adsorption–desorption cycles, over 85% recovery ratio was attained, indicating the high regeneration capacity of Fe_3O_4/HA.

4. Conclusion

Fe_3O_4/HA was prepared from coprecipitation procedure with iron salts and HA, and its properties for removal of RhB from aqueous solution was investigated. TEM images revealed the Fe_3O_4/HA (with ~10 nm Fe_3O_4 cores) were aggregated as aqueous suspensions. With a saturation magnetization of 61.2 emu/g, the Fe_3O_4/HA could be simply re-collected from water with magnetic separations at low magnetic field gradients within a few minutes. Sorption of the RhB to Fe_3O_4/HA reached equilibrium in less than 15 min, and agreed well to the Langmuir adsorption model with maximum adsorption capacities of 161.8 mg/g. The effect of temperature revealed that the adsorption of the dye, RhB is an exothermic, but the adsorption is enhanced as increasing temperature from 20 to 70 °C. The Fe_3O_4/HA was able to remove 98.5% of RhB in water at pH 2.53, and this adsorbent was stable in solution with low pH. The magnetic Fe_3O_4/HA is a potential high efficient nanomaterial for removal of RhB from water body.

Acknowledgments

For the financial support we are grateful to the National Natural Science Foundation of China (No. 21007014, 21107024), the Start Foundation of Hunan Agricultural University (No. 10YJ01), the National Science and Technology Major Projects (2009ZX07212-001-05), the National Environmental Protection Public Welfare Program (No. 201009047) and Key Laboratory of Production Environment and Agro-product Safety of Ministry of Agriculture, Tianjin Key Laboratory of Agro-environment and Food Safety (2010-KJ-KF-03) and Scientific Research Fund of Hunan Provincial Education Department (11C0650).

References

[1] V.K. Garg, M. Amita, R. Kumar, R. Gupta, Basic dye (methylene blue) removal from simulated wastewater by adsorption using Indian rosewood saw dust: a timber industry waste, Dyes Pig. 63 (3) (2004) 243–250.
[2] R. Malik, D.S. Ramteke, S.R. Wate, Adsorption of malachite green on ground nut shell waste based powdered activated carbon, Waste Manage. 27 (9) (2007) 1129–1138.
[3] H.M.H. Gad, A.A. El-Sayed, Activated carbon from agricultural by-products for the removal of Rhodamine-B from aqueous solution, J. Hazard. Mater. 168 (2–3) (2009) 1070–1081.
[4] F. Ferrero, Adsorption of methylene blue on magnesium silicate: kinetics, equilibria and comparison with other adsorbents, J. Environ. Sci. 22 (3) (2010) 467–473.
[5] L. Li, S. Liu, T. Zhu, Application of activated carbon derived from scrap tires for adsorption of Rhodamine B, J. Environ. Sci. 22 (8) (2010) 1273–1280.
[6] S.H. Chang, K.S. Wang, H.C. Li, M.Y. We, J.D. Chou, Enhancement of Rhodamine B removal by low-cost fly ash sorption with Fenton pre-oxidation, J. Hazard. Mater. 172 (2–3) (2009) 1131–1136.
[7] K. Zhao, G. Zhao, P. Li, J. Gao, B. Lv, D. Li, A novel method for photodegradation of high-chroma dye wastewater via electrochemical pre-oxidation, Chemosphere 80 (4) (2010) 410–415.
[8] J. Rajeev, M. Megha, S. Shalini, M. Alok, Removal of the hazardous dye Rhodamine B through photocatalytic and adsorption treatments, J. Environ. Manage. 85 (4) (2007) 956–964.
[9] F. Ma, H. Tan, Adsorption decolorization of CMC-g-CPAM to reactive dyestuffs, Dye. Finish. 32 (15) (2006) 14–15.
[10] J. Teng, J. Xu, Research on the adsorption of Rhodamine 6G by vermiculite, Guangdong Chemical Industry 37 (3) (2010) 81–82.
[11] R. Lei, C. Shi, S. Liu, A Study on adsorption of kaolinite on Rhodamine B and photo-Fenton degradation, J. Univ. Sci. Technol. Suzhou Eng. Technol. 22 (3) (2009) 17–21.
[12] M. Hou, C. Ma, W. Zhang, X. Tang, Y. Fan, H. Wan, Removal of rhodamine B using iron-pillared bentonite, J. Hazard. Mater. 186 (2–3) (2011) 1118–1123.
[13] D. Maity, D.C. Agrawal, Synthesis of iron oxide nanoparticles under oxidizing environment and their stabilization in aqueous and non-aqueous media, J. Magn. Magn. Mater. 308 (1) (2007) 46–55.
[14] Y. Lin, H. Chen, K. Lin, B. Chen, C. Chiou, Application of magnetic particles modified with amino groups to adsorb copper ions in aqueous solution, J. Environ. Sci. 23 (1) (2011) 44–50.
[15] C.L. Warner, R.S. Addleman, A.D. Cinson, T.C. Droubay, M.H. Engelhard, M.A. Nash, W. Yantasee, M.G. Warner, High-performance, superparamagnetic, nanoparticle-based heavy metal sorbents for removal of contaminants from natural waters, ChemSusChem. 3 (6) (2010) 749–757.
[16] E. Ills, E. Tombacz, The role of variable surface charge and surface complexation in the absorption of humic acid on magnetite, Colloids Surf. A 230 (2003) 99–109.
[17] E. Ills, E. Tombacz, The effect of humic acid adsorption on pH-dependent surface charging and aggregation of magnetite nanoparticles, J. Colloid Interface Sci. 295 (1) (2006) 115–123.
[18] J. Liu, Z. Zhao, G. Jiang, Coating Fe_3O_4 magnetic nanoparticles with humic acid for high efficient removal of heavy metals in water, Environ. Sci. Technol. 42 (18) (2008) 6949–6954.
[19] W. Yantasee, C.L. Warner, T. Sangvanich, R.S. Addleman, T.G. Carter, R.J. Wiacek, G.E. Fryxell, C. Timchalk, M.G. Warner, Removal of heavy metals from aqueous systems with thiol functionalized superparamagnetic nanoparticles, Environ. Sci. Technol. 41 (14) (2007) 5114–5119.
[20] B. Gu, J. Schmitt, Z. Chen, L. Liang, J.F. Carthy, Adsorption and desorption of natural organic matter on iron oxide: mechanisms and models, Environ. Sci. Technol. 28 (1) (1994) 38–46.
[21] R.A. Alvarez-Puebla, J.J. Garrido, Effect of pH on the aggregation of a gray humic acid in colloidal and solid states, Chemosphere 59 (5) (2005) 659–667.
[22] R.A. Alvarez-Puebla, P.J.G. Goulet, J.J. Garrido, Characterization of porous structure of different humic fractions, Colloids Surf. A 256 (2–3) (2005) 129–135.
[23] A.V. Deshpande, U. Kumar, Effect of method of preparation on photophysical properties of Rh-B impregnated sol–gel hosts, J. Non-Cryst. Solids 306 (2) (2002) 149–159.
[24] C.H. Giles, T.H. Macewan, S.N. Nakhwa, D. Smith, Studies in adsorption. Part XI. A system of classification of solution adsorption isotherms, and its use in diagnosis of adsorption mechanisms and in measurements of specific surface areas of solids, J. Chem. Soc. 10 (3) (1960) 3973–3993.